AN INTERFEROMETRIC METHOD FOR THE SIMULTANEOUS

MEASUREMENT OF HEAT AND MASS TRANSFER

A THESIS

Presented to

The Faculty of the Division of Graduate

Studies and Research

By

James Stewart Morris

In Partial Fulfillment

of the Requirements for the Degree

Master of Science in Mechanical Engineering

Georgia Institute of Technology

August, 1974

AN INTERFEROMETRIC METHOD FOR THE SIMULTANEOUS

MEASUREMENT OF HEAT AND MASS TRANSFER

Approved:

William Z. Black, Chairman

Charles W. Gorton

Michael J. Matteson

Date approved by Chairman: 8/8/74

ACKNOWLEDGMENTS

I wish to express my gratitude and appreciation to my advisor, Dr. William Z. Black, for his guidance, encouragement, understanding, and professional advice throughout the work leading to completion of this thesis. I also thank the members of my reading committee, Dr. C. W. Gorton and Dr. M. J. Matteson for their advice and corrections.

The assistance of Mr. T. E. Clopton in setting up the temperature measurement and recording equipment is greatly appreciated. The author would also like to thank Dr. Chuck Carr and Mr. Robert Somers for their helpful suggestions during the work of this thesis.

Finally, the guidance, patience, and encouragement of the author's parents is greatly appreciated.

TABLE OF CONTENTS

LIST OF TABLES

LIST OF ILLUSTRATIONS

NOMENCLATURE

Symbol	Definition	Units
c	Molar density	$gm\text{-}moles/cm^3$
c_{PA}	Specific heat at constant pressure of the vapor of the evaporating liquid	$gm\text{-}cm^2/sec^2 mole\ ^oK$
D_{AB}	Mass diffusivity	cm^2/sec
g	Distance between first Wollaston prism and spherical mirror	cm
$\bar{g}$	Acceleration of gravity	cm/sec^2
h	Distance above evaporating surface where the temperature is known	cm
H	Distance from evaporating surface to top of test cell	cm
k	Thermal conductivity	$gm\text{-}cm/sec^3\ ^oK$
L	Length of light path through test cell	cm
m	Number of fringe shifts	Dimensionless
M	Molecular weight	$gm/gm\text{-}mole$
n	Index of refraction	Dimensionless
n_{DB}	Index of refraction of dry air	Dimensionless
n_e	Extraordinary index of refraction of birefrigent material	Dimensionless
n_o	Ordinary index of refraction of birefrigent material	Dimensionless
N	Molar refractivity	$cm^3/gm\text{-}mole$
N_{AZ}	Molar flux	$moles/cm^2\ sec$
p	Pressure	atm, mm of Hg

Symbol	Definition	Units
P	Pressure	atm, mm of Hg
P_V	Vapor pressure of diffusing substance	atm, mm of Hg
q''	Heat flux	$cal/cm^2 sec$
$\bar{R}$	Universal gas constant	$cm^3 atm/gm\text{-}mole\ ^\circ K$
T	Temperature	$^\circ K$
T_h	Temperature at a distance h above the evaporating surface	$^\circ K$
T_s	Temperature at the evaporating surface	$^\circ K$
v	Velocity	cm/sec
x	Mole fraction	Dimensionless
z	Coordinate perpendicular to evaporating surface	cm

Greek Symbols

β	Coefficient of thermal expansion	$^\circ F^{-1}$
δ	Distance above evaporating surface where the temperature is known	cm
θ	Wollaston prism angle	Radians
λ	Wavelength	Angstroms
μ	Viscosity	gm/cm sec
ν	Kinematic viscosity	ft^2/sec
ρ	Density	gm/cm^3
σ	Lennard-Jones force constant	Angstroms
Ω	Lennard-Jones potential function	Dimensionless

Subscripts

A	Property of diffusing substance
AO	Property of substance A at the surface

Symbol	Definition
AH	Property of substance A at a distance H above evaporating surface
B	Property of air
wv	Property of water vapor in the air
z	Quantity in z direction

Superscript

| o | Signifies heat transfer with no mass transfer |

SUMMARY

This thesis describes the application of a differential inter-
ferometer to the measurement of simultaneous heat and mass transfer for
one-dimensional binary gas diffusion in free convection. An equation
existed which related the interferometer fringe shift measurement to the
temperature and concentration gradients. The major effort of this thesis
was to derive a second, independent, non-interferometric equation which
provided a relationship between the two unknowns, temperature gradient
and concentration gradient. Once this was accomplished, the two indepen-
dent equations were combined so that a single interferometer fringe shift
measurement provided simultaneous measurements of the heat and mass trans-
fer rates. The second equation was obtained by combining the equation of
state and the conservation of mass and energy equations.

The test equipment consisted of a differential interferometer with
three Wollaston Prisms, a diffusion test cell with a heater, a special
temperature control device, temperature measurement equipment and a 4 inch
by 5 inch still camera. The test cell was constructed to model one-dimen-
sional binary gas diffusion in free convection.

Preliminary tests were run to verify that the interferometer could
measure heat transfer without mass transfer, and also mass transfer without
heat transfer. The results obtained with the interferometer were compared
with a theoretical model. For heat transfer only the interferometer pro-
vided a temperature gradient which was 12.8% less than that predicted by

theory. For mass transfer the interferometer yielded a concentration gradient which was 3% less than that predicted by theory.

The results of three simultaneous heat and mass transfer tests were presented. A theoretical check of these results was not made because the theoretical model for simultaneous heat and mass transfer was limited to many simplifying assumptions that made comparison impractical. One of the three tests was repeated four times with insignificant differences in the results which verified repeatability.

CHAPTER I

INTRODUCTION AND BACKGROUND

Simultaneous heat and mass transfer is an extremely difficult problem area in which to study, but one which has many industrial applications. Typical processes which involve combined heat and mass transfer include: absorption, adsorption, distillation, desorption, humidification, dehumidification and many others. Hence the design of equipment which involves both heat and mass transfer such as spray towers, cooling towers, distillation equipment, dehumidifying equipment, continuous dryers and others require a basic understanding of combined heat and mass transfer.

An analytical solution to the general problem of simultaneous heat and mass transfer is limited to only the simplest geometries and it must be restricted by numerous simplifying assumptions. Often times the simplifying assumptions destroy a degree of realism in the physical problem. Even if the governing constitutive equations can be formulated, it may be impractical to obtain an analytical solution or extremely time consuming to numerically approximate the solution.

Since analytical solutions are so restricted, experimental techniques are attempted in order to provide an understanding of the combined heat and mass transfer process. The work done in the experimental area using interferometers will be discussed.

The ability of an interferometer to provide data on concentration and temperature distributions makes it an extremely useful tool in the

experimental study of the combined process. Interferometers provide accuracy, sensitivity and the ability to respond to cases of rapidly changing flow phenomena. Some attempts have been made to measure simultaneous heat and mass transfer using interferometers, but so far with no reasonable success. The attempts made thus far have been with the Mach Zehnder or similar type interferometers and are now discussed.

Ross and El-Wakil [1] in 1960 used a two wavelength interferometric technique for the study of vaporization and combustion of fuels. An equation was developed which related the Mach-Zehnder interferometer fringe shift measurement to the temperature and concentration gradients. The two gradients were a function of the wavelength and hence two filters were chosen with wavelengths as far apart as possible, but still within the visible range. During a particular test, pictures were taken of the resulting fringe deflection at two different wavelengths. Since the two gradients were closely dependent upon each other, and did change rapidly with time, the simultaneous fringe shift measurements at the two wavelengths was essential. Because the variation of the molar refractivities with respect to wavelength is small within the visible spectrum for most vapors and gases of interest, the experimental technique did not provide satisfactory sensitivity. This method resulted in two equations in the two unknowns, concentration gradient and temperature gradient, but since the two wavelengths did not provide drastically different properties, the two equations were almost identical making a simultaneous solution of the two equations impractical. Furthermore the two wavelength technique suffered a problem from the requirement of photographing the interference pattern simultaneously at two different wavelengths.

In 1964 El-Wakil and Jaeck [2] applied a two wavelength Mach-Zehnder interferometer technique to a cylindrical diffusing surface. Again it was concluded that the method could only be used when the diffusing gases had molar refractivities which varied greatly with wavelengths so that the two equations could be accurately solved for the temperature and concentration profiles.

Sadovnikov, Smol'skiy and Shchitnikov [3] in 1969 used a IZK-454 interferometer which was manufactured in the Soviet Union. Again the investigation involved the use of two wavelengths for determining the two independent equations in temperature and concentration gradients. It was concluded that the IZK-454 interferometer was also capable of measuring the temperature and concentration gradients simultaneously provided the gases have widely varying molar refractivities with respect to wavelength. It was also concluded that the simultaneous recording of the fringe shift pattern at two different wavelengths presented problems.

Based on the problems with the two wavelength technique, Prasad, Chen and Beard [4] in 1970 developed a one wavelength technique with the addition of a noninterferometric measurement of temperature or concentration. An interferometric equation was developed which related the temperature and concentration to the fringe shift. The temperature or concentration was measured by means of a thermocouple or hygrosensor, respectively. This conventionally measured value of temperature or concentration was then substituted into the interferometer equation along with the fringe shift measurement to determine the other unknown. Both methods were attempted, and it was concluded that better results were obtained by measuring the temperature by a conventional method, and then using the interferometer

equation to evaluate the concentration. It was also concluded that concentration gradients have a larger effect on fringe shift as compared to the effect of temperature alone. It was concluded that the single wavelength technique had an advantage over the two wavelength technique in that it was not necessary with the one wavelength technique to have gases with widely varying molar refractivities with respect to wavelength.

The experimental work in the area of simultaneous measurements of heat and mass transfer rates has used primarily the Mach-Zehnder or similar type interferometers. The Mach-Zehnder interferometer produces fringe lines which are identical to isotherms for heat transfer or lines of constant concentration for mass transfer. In order to find the temperature gradient for example one must approximate the temperature gradient by knowing the location of the isotherms. In this respect the differential interferometer has a tremendous advantage over the Mach-Zehnder interferometer, because the differential interferometer produces a fringe shift which is directly proportional to the index of refraction gradient. Since the index of refraction gradient can be directly related to the temperature and concentration gradients, the differential interferometer produces an interferogram that is a direct measurement of the simultaneous heat and mass transfer rates. The relatively new differential interferometer has not been used as yet for the study of simultaneous heat and mass transfer.

Previous efforts [5] have resulted in an equation which relates the

differential interferometer fringe shift to the combined effects of a temperature and concentration gradient. This equation has been applied to problems involving heat transfer without mass transfer and to isothermal mass transfer. No previous effort has been made to use this equation to provide a measurement of both heat and mass transfer rates while both diffusion processes are occurring simultaneously. The reason is because a single fringe shift measurement is incapable of distinguishing which portion of the fringe shift deflection is caused by each gradient. The two factors which cause ray retardation which results in a fringe pattern can only be separated if a second independent equation can be derived which ralates the two gradients.

The major effort of this thesis will be to derive a second independent equation by combining the equation of state and the conservation of mass, momentum and energy equations resulting in a functional relationship between the temperature and concentration gradients. Upon combining the interferometer equation with the equation derived in this thesis, a single measurement of the fringe shift will provide the temperature and concentration gradients simultaneously. Experiments will then be performed to verify that the differential interferometer can accurately measure the temperature and concentration gradients independently. The accuracy of the method will be checked by comparing the experimental results with theoretical calculations. Finally measurements will be made of simultaneous heat and mass transfer of a liquid under conditions of one dimensional binary gas diffusion in free convection.

CHAPTER II

THEORETICAL DEVELOPMENT

The process of simultaneous heat and mass transfer under consideration involves evaporation of a liquid from a heated horizontal liquid surface. The process is assumed to be one dimensional binary gas diffusion and the transfer of heat is assumed to be by free convection. See Figure 1 for the test cell geometry. Both the temperature and concentration gradients at the liquid surface will be determined simultaneously as a function of a single interferogram fringe shift measurement. Once the gradients have been determined, the heat and mass fluxes will be found by the use of the Fourier Biot Law and Fick's Law of Diffusion.

The differential interferometer produces fringe patterns for which the deflection of a single fringe shift is proportional to the gradient in the index of refraction. The index of refraction for a gas is dependent upon the gas concentration, the gas temperature and the wavelength of light used to produce the fringe pattern. Therefore, whenever a region under observation contains a non-isothermal gas that varies in concentration, the resulting interference pattern is a record of the combined effects of the temperature and concentration gradients. Since the heat and mass transfer rates are directly proportional to these gradients, the fringe deflection produced is a measure of the simultaneous transfer of both heat and mass.

A relationship between the fringe shift of the interference pattern (m), the temperature gradient $(\frac{\partial T}{\partial z})$, the concentration gradient $(\frac{\partial c_A}{\partial z})$ and
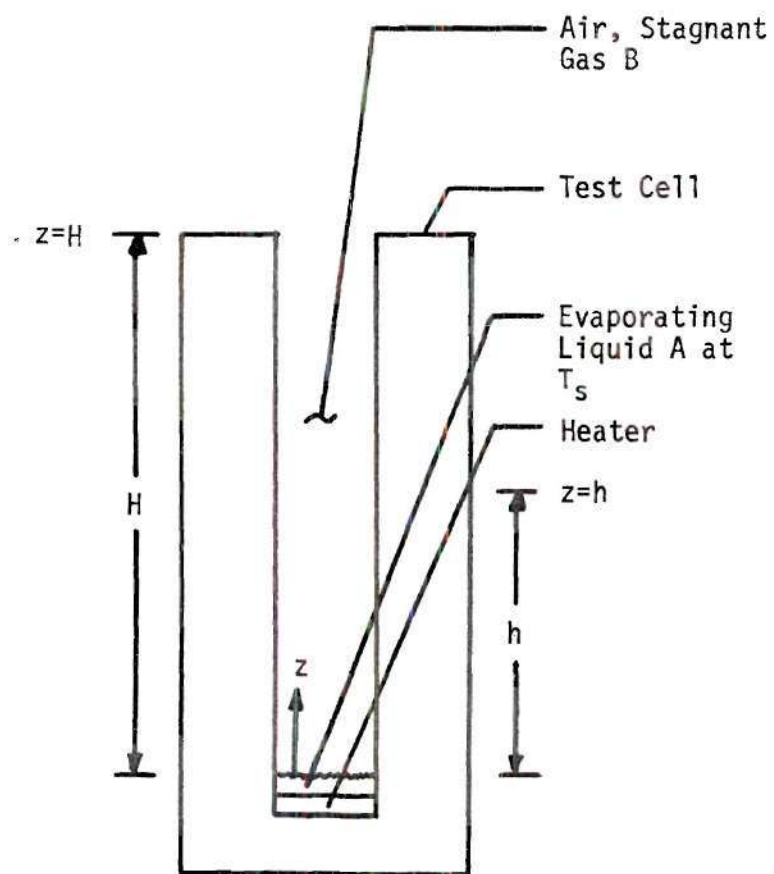
Figure 1. Test Cell Geometry for One-Dimensional
Binary Gas Diffusion in Free Convection.

various optical properties of the interferometer has been previously derived in Reference [5]. The derivation assumes gas A diffusing into a second gas B both of which are ideal. The gases are not isothermal although the total pressure is assumed constant. The relationship is

$$m = \frac{3Lg\theta(n_e - n_o)}{\lambda} \left[(N_A - N_B) \frac{\partial c_A}{\partial z} - \frac{N_B P}{RT^2} \frac{\partial T}{\partial z} \right] \qquad (II-1)$$

where N_A and N_B are the molar refractivities of the two gases and the term $\left[\frac{g\theta(n_e - n_o)}{\lambda} \right]$ is a function of the optical settings of the interferometer. For the purposes of discussion this term may be assumed to be constant.

Equation (II-1) indicates that a single fringe shift deflection measurement by itself is not sufficient for the independent determination of both gradients since there are two unknowns: $\frac{\partial c_A}{\partial z}$ and $\frac{\partial T}{\partial z}$. Therefore, another equation must be derived for this purpose. An equation involving the two gradients results by combining the equation of state and the governing conservation of mass, momentum and energy equations. Once this has been accomplished, then a single fringe shift measurement will indeed provide a measure of both heat and mass transfer in a binary gas system. This equation is derived in Section A of this chapter. The two special cases of isothermal mass transfer, and heat transfer without evaporation are derived in Section B of this chapter. These results will be used to verify the interferometer equation for the two simplified cases.

A. Simultaneous Heat and Mass Transfer

The following derivation relating the temperature and concentration

gradients is based on a one-dimensional model involving binary gas diffusion and simultaneous heat transfer by free convection. Other assumptions used during the derivation are:

a. One-dimensional (z direction) heat and mass transfer

b. Steady state conditions prevail

c. Binary gas diffusion where both the diffusing gas A and the stagnant gas B obey the ideal equation of state and are Newtonian

d. Total pressure is constant

e. Liquid surface is isothermal at T_s.

f. Radiant heat transfer is negligible.

g. Thermal diffusion is negligible.

h. Species B is insoluble in liquid A.

i. No chemical reactions occur.

Two methods of finding the needed second independent equation $\frac{\partial T}{\partial z} = f(\frac{\partial c_A}{dz})$ were investigated. Even though only one method proved to be satisfactory both methods are presented here for completeness.

1. Method I

The first method involved the idea of combining the equation of state and the governing conservation of mass, momentum and energy equations to obtain one equation involving the two unknowns ($\frac{dT}{dz}$ and $\frac{dc_A}{dz}$). The assumptions given earlier in the chapter are assumed to be valid for this problem. In addition the physical properties are not assumed to be constants. The thermal conductivity, specific heat at constant pressure and viscosity are all functions of both concentration and temperature. The mass diffusivity (D_{AB}) for binary mixtures at low pressures is a function

of temperature only. The advantage of this method is that one only needs to know the boundary conditions and physical properties at the surface to evaluate the resulting equation.

The four main equations used for the derivation are:

1. Equation of State

$$P = c\bar{R}T \tag{II-2}$$

2. Conservation of Momentum
(Reference 7, eq. 3.2-19)

$$\rho v_z \frac{\partial v_z}{\partial z} = \frac{\partial}{\partial z}\left(\frac{4}{3}\mu \frac{\partial v_z}{\partial z}\right) + \rho \bar{g}_z \tag{II-3}$$

3. Conservation of Mass
(Reference 7, eq. 18.5-1)

$$\frac{dN_{AZ}}{dz} = 0 \tag{II-4}$$

4. Conservation of Energy
(Reference 7, eq. 18.5-2 and 18.5-7)

$$\frac{d}{dz}\left(-k\frac{dT}{dz}\right) + \frac{d}{dz}\left(N_{AZ}c_{PA}(T - T_0)\right) = 0 \tag{II-5}$$

Note: T_0 is the reference temperature for enthalpy.

The above conservation equations are second order in both temperature and concentration so unknown terms like $\frac{d^2T}{dz^2}$, $\frac{d^2c}{dz^2}$, $\frac{dc}{dz}$ and $\frac{d^2c_A}{dz^2}$ had to be eliminated by combining the above equations.

Several other supplementary equations are needed before the final

equation relating the two unknown gradients can be written. These equations are:

1. Mass Average Velocity
   (Reference 7, p. 498)

$$v_Z = \frac{\rho_A}{\rho} v_{AZ} + \frac{\rho_B}{\rho} v_{BZ}$$

(II-6)

2. Mass Flux of Species A
   (Reference 7, p. 499)

$$n_{AZ} = \rho_A v_{AZ}$$

(II-7)

3. Equation Relating the Mass Flux to Molar Flux
   (Reference 7, p. 499)

$$n_{AZ} = N_{AZ} M_A$$

(II-8)

4. Molar Flux of Species A
   (Reference 7, eq. 18.5-3)

$$N_{AZ} = - \frac{c D_{AB}}{1-x_A} \frac{dx_A}{dz}$$

(II-9)

5. Mole Fractions

$$x_A = \frac{c_A}{c} \quad \text{and} \quad x_B = \frac{c_B}{c}$$

(II-10)

6. Molar Density of Mixture

$$c = c_A + c_B$$

(II-11)

7. Mass Density of Mixture

$$\rho = c_A M_A + c_B M_B$$

(II-12)

8. Viscosity of Mixture
   (Reference 7, eq. 1.3-5)

$$\mu = x_A \mu_A(T) + x_B \mu_B(T) \tag{II-13}$$

9. Thermal Conductivity of Mixture

$$k = x_A k_A(T) + x_B k_B(T) \tag{II-14}$$

10. Chain Rule of Calculus

$$\frac{\partial k_A}{\partial z} = \frac{\partial k_A}{\partial T} \frac{\partial T}{\partial z} \tag{II-15}$$

Note: Similar expressions can be written for k_B, μ_A, μ_B and D_{AB}.

When equations (II-2) through (II-15) were combined, a third degree algebraic equation relating the two gradients of the following form resulted

$$B_1 \left(\frac{\partial T}{\partial z}\right)^3 + B_2 \left(\frac{\partial c_A}{\partial z}\right)^3 + B_3 \left(\frac{\partial T}{\partial z}\right)^2 \left(\frac{\partial c_A}{\partial z}\right) + B_4 \left(\frac{\partial c_A}{\partial z}\right)^2 \left(\frac{\partial T}{\partial z}\right) + B_5 = 0 \tag{II-16}$$

A complete listing of the coefficients B_1 through B_5 is given in Appendix A. These coefficients contained combinations of the following terms: M_A, M_B, ρ, T, c, c_A, c_{PA}, D_{AB}, $\frac{\partial D_{AB}}{\partial T}$, k, k_A, $\frac{\partial k_A}{\partial T}$, μ, μ_A, $\frac{\partial \mu_A}{\partial T}$, μ_B, $\frac{\partial \mu_B}{\partial T}$ and $\bar{g}_z$. As can be seen the B coefficients were extremely complicated, but could all be determined at the surface once the surface temperature T_s is known. Hence, equation (II-16) is an equation which can be used to relate the two unknowns ($\frac{dT}{dz}$ and $\frac{dc_A}{dz}$) at the liquid interface.

Various procedures were used to check and to simplify equation (II-16). A dimensional check proved satisfactory. Next, the equation

was non-dimensionalized. Then an order of magnitude analysis was performed on each term in the equation in an attempt to eliminate the smallest terms. Due to the complexity of the equation the magnitude analysis could not be performed by hand. Finally a computer program was written to calculate all of the B coefficients. The program included a subroutine to calculate the derivatives of the properties k_A, k_B, μ_A, μ_B and D_{AB} with respect to temperature. The results of this attempt showed that all of the individual terms which make up each B coefficient were of the same order of magnitude and all were extremely small.

Since the order of magnitude results indicated that all terms were of the same relative magnitude, the equation (II-16) could not be simplified further. The complete equation was programmed for a solution on a digital computer. To check the solution a simplified case of simultaneous heat and mass transfer was used to input known values of the temperature and concentration gradients. A value for the concentration gradient was selected and equation (II-16) was used to produce a value for the temperature gradient. These values were checked with gradients that were known to exist from an experimental investigation. The values of the gradients resulting from the computer program did not coincide with the experimental results.

At this point the formation of equation (II-16) and the assumptions used in its derivation were reviewed. It was concluded that the use of the momentum equation was the cause of the small terms. Since all of the terms in the momentum equation were small and of the same order as terms such as $-\frac{\partial p}{\partial z}$ which had been previously neglected, none of the terms

should have been dropped from equation 3.2-19 of Reference 7. The term $-\frac{\partial p}{\partial z}$ was dropped initially because of the assumption that the total pressure was constant. If this term could not be neglected, it would create another unknown, namely the pressure gradient, which would make the solution impossible. Hence, it was concluded that this particular method was not capable of producing the needed second equation in $\frac{dT}{dz}$ and $\frac{dc_A}{dz}$.

2. Method II

The second method involved the combination of the equation of state and the conservation of mass and energy equations. This analysis does not use the conservation of momentum equation. It does, however, require that the temperature a distance h above the surface be known. Again the assumptions given in the first part of the chapter (page 9) are applicable to the derivation used in this method. In addition the physical properties are assumed to be constant.

The conservation of energy equation is

$$\frac{d}{dz}\left(-k\frac{dT}{dz} + N_{AZ}c_{PA}(T - T_o)\right) = 0 \tag{II-17}$$

(Reference 7, eqs. 18.5-2 and 18.5-7)

where T_o is the enthalpy reference temperature. Since it is assumed that k and c_{PA} are constant and N_{AZ} is known to not vary with z, differentiation of equation (II-17) gives

$$\frac{d^2T}{dz^2} - \frac{N_{AZ}c_{PA}}{k}\frac{dT}{dz} = 0 \tag{II-18}$$

The boundary conditions are

$$\text{B.C.1} \quad \text{at } z = 0, \quad T = T_s$$

$$\text{B.C.2} \quad \text{at } z = h, \quad T = T_h$$

The general form of the solution to equation (II-18) is

$$T = C_1 \exp\left(\frac{N_{AZ}c_{PA}}{k}\right) + C_2 \tag{II-19}$$

where C_1 and C_2 are constants of integration. Substitution of the two boundary conditions into equation (II-19) yields

$$T = \frac{T_s - T_h}{1 - \exp\left(\frac{N_{AZ}c_{PA}}{k} h\right)} \exp\left(\frac{N_{AZ}c_{PA}}{k} z\right) + T_s - \frac{T_s - T_h}{1 - \exp\left(\frac{N_{AZ}c_{PA}}{k} h\right)} \tag{II-20}$$

To determine the temperature gradient, equation (II-20) is differentiated with respect to z to give

$$\frac{dT}{dz} = - \frac{\frac{N_{AZ}c_{PA}}{k}(T_h - T_s)\exp\left(\frac{N_{AZ}c_{PA}}{k} z\right)}{1 - \exp\left(\frac{N_{AZ}c_{PA}}{k} h\right)} \tag{II-21}$$

The temperature gradient at the surface where $z = 0$ is

$$\left.\frac{dT}{dz}\right|_{z=0} = - \frac{\frac{N_{AZ}c_{PA}}{k}(T_h - T_s)}{1 - \exp\left(\frac{N_{AZ}c_{PA}}{k} h\right)} \tag{II-22}$$

Before equation (II-22) can be used as the required relationship between temperature and concentration gradients, the molar flux N_{AZ} must be expressed in terms of c_A, $\frac{dc_A}{dz}$ and $\frac{dT}{dz}$. This expression may be

obtained by combining the molar flux equation

$$N_{AZ} = - \frac{cD_{AB}}{1 - x_A} \frac{dx_A}{dz}$$

(II-23)

the definition of mole fraction

$$x_A = \frac{c_A}{c}$$

(II-24)

and the ideal equation of state

$$c = \frac{P}{\overline{R}T}$$

(II-25)

The derivative of equation (II-24) with respect to z gives

$$\frac{dx_A}{dz} = \frac{1}{c} \frac{\partial c_A}{\partial z} - \frac{c_A}{c^2} \frac{\partial c}{\partial z}$$

(II-26)

and the derivative of equation (II-25) with respect to z gives

$$\frac{dc}{dz} = - \frac{P}{\overline{R}T^2} \frac{dT}{dz}$$

(II-27)

Upon substituting equations (II-24), (II-26) and (II-27) into equation (II-23) the following expression is obtained for N_{AZ}

$$N_{AZ} = - \frac{D_{AB}}{c-c_A} [c \frac{\partial c_A}{\partial z} + \frac{c_A P}{\overline{R}T^2} \frac{\partial T}{\partial z}]$$

(II-28)

The interferometer equation (II-1) is solved for $\frac{dc_A}{dz}$ at the surface to give

$$\frac{dc_A}{dz} \bigg|_{z=0} = \frac{N_B P}{\overline{R}T^2 (N_A - N_B)} \frac{dT}{dz} \bigg|_{z=0} + \frac{m\lambda}{3Lg\theta (n_e - n_o)(N_A - N_B)}$$

(II-29)

Equations (II-28) and (II-29) are substituted into equation (II-22) and after much rearranging the following equation results for the temperature gradient at the surface

$$\frac{dT}{dz}\bigg|_{z=0} [-(A_1+A_2) + 1 - \exp [-(A_6+A_4) \frac{dT}{dz}\bigg|_{z=0} - A_5]] - A_2 = 0 \quad (II-30)$$

where the terms A_1 through A_6 are given as follows

$$A_1 = \frac{D_{AB}c_{PA}c(T_h-T_s)N_B P}{k(c-c_A)\bar{R}\, T_s^2(N_A-N_B)} \quad (II-31)$$

$$A_2 = \frac{D_{AB}c_{PA}c(T_h-T_s)m\lambda}{3k(c-c_A)Lg\theta(n_e-n_o)(N_A-N_B)} \quad (II-32)$$

$$A_3 = \frac{D_{AB}c_{PA}c_A P(T_h-T_s)}{k(c-c_A)\bar{R}\, T_s^2} \quad (II-33)$$

$$A_4 = \frac{D_{AB}c_{PA}h\, c\, N_B P}{k(c-c_A)\bar{R}\, T_s^2(N_A-N_B)} \quad (II-34)$$

$$A_5 = \frac{D_{AB}c_{PA}h\, c\, m\lambda}{3k(c-c_A)Lg\theta(n_e-n_o)(N_A-N_B)} \quad (II-35)$$

$$A_6 = \frac{D_{AB}c_{PA}h\, c_A P}{k(c-c_A)\bar{R}\, T_s^2} \quad (II-36)$$

Equations (II-31) through (II-36) consist of known optical, physical and thermodynamic properties of the gases, parameters fixed by various adjustments of the interferometer, the measured temperature T_s at the

evaporating surface, the measured temperature T_h at a distance h above the evaporating surface and the measured fringe shift m. Hence, equations (II-31) through (II-36) can be evaluated for a given test and fringe shift measurement. These six known values for the coefficients A_1 through A_6 can provide a value for the temperature gradient $\frac{dT}{dz}\Big|_{z=0}$ at the surface from equation (II-30). The concentration gradient at the surface can then be determined by equation (II-29). A single fringe shift measurement m along with the corresponding values for the optical and physical properties will therefore provide a measure of the temperature and concentration gradients given by equations (II-30) and (II-29), respectively.

B. Special Cases

The interferometer equation (II-1) was checked for the two special simplified cases of isothermal mass transfer, and heat transfer without evaporation. Theoretical equations will be developed for the two special cases so that experimental results from the interferometer for $\frac{dc_A}{dz}$ without heat transfer, and $\frac{dT}{dz}$ without evaporation can be verified. By checking these independent experimental results with theory it can be determined that the differential interferometer can measure temperature and concentration gradients independently, and, therefore, show that equation (II-1) is indeed valid for this study.

1. Isothermal Mass Transfer

It will be shown experimentally that the interferometer can measure the concentration gradient at the surface under conditions of one-dimensional binary gas diffusion with no heat transfer. The geometry

is similar to Figure 1. For this case where $\frac{dT}{dz} = 0$, equation (II-1) reduces to

$$\frac{dc_A}{dz}\bigg|_{z=0} = \frac{m}{3Lg\theta(n_e-n_o)(N_A-N_B)} \tag{II-37}$$

This equation implies that the single measurement of the fringe shift m provides the concentration gradient directly, and hence the mass flux at the surface. In order to verify this, a theoretical check for the experimental results provided by equation (II-37) will be derived.

In this particular case we have binary gas diffusion where liquid A is evaporating into gas B. At the liquid-gas interface the gas-phase concentration of A, expressed as a mole fraction, is x_{AO}. Assuming that A and B form an ideal gas mixture, x_{AO} can be expressed as the vapor pressure of A divided by the total pressure of the mixture.

When the system attains steady state, there is a net motion of A away from the evaporating surface and the vapor B is stationary. Hence the equation given in Reference 7 (page 523)

$$N_{AZ} = -\frac{cD_{AB}}{1-x_A}\frac{dx_A}{dz} \tag{II-38}$$

can be used to relate the molar flux to the gradient of the mole fraction. Since N_{AZ} remains constant for any given cross-section over the test section height, the conservation of mass equation may be expressed as

$$\frac{dN_{AZ}}{dz} = 0 \tag{II-39}$$

Substitution of equation (II-38) into (II-39) gives

$$\frac{d}{dz}\left(\frac{cD_{AB}}{1-x_A}\frac{dx_A}{dz}\right) = 0 \qquad (II-40)$$

For ideal gas mixtures at constant temperature and pressure, c is a constant, and D_{AB} is nearly independent of concentration as stated in Reference 7 (page 524). Hence, equation (II-40) becomes

$$\frac{d}{dz}\left(\frac{1}{1-x_A}\frac{dx_A}{dz}\right) = 0 \qquad (II-41)$$

Integration with respect to z yields

$$\frac{1}{1-x_A}\frac{dx_A}{dz} = c_1 \qquad (II-42)$$

A second integration gives

$$-\ln(1-x_A) = c_1 z + c_2 \qquad (II-43)$$

The constants of integration (c_1 and c_2) may be determined by the use of the following boundary conditions

B.C. 1   at $z = 0$, $x_A = x_{A0}$

B.C. 2   at $z = H$, $x_A = x_{AH}$

Applying B.C. 1 gives

$$-\ln(1-x_{A0}) = c_2 \qquad (II-44)$$

Applying B.C. 2 gives

$$c_1 = \frac{1}{H}\ln\left(\frac{1-x_{A0}}{1-x_{AH}}\right) \qquad (II-45)$$

Substituting c_1 into equation (II-42) yields the following result for the

first derivative of the mole fraction of A

$$\frac{dx_A}{dz} = \frac{1-x_A}{H} \ln \left(\frac{1-x_{A0}}{1-x_{AH}}\right) \qquad (II-46)$$

In order to convert the first derivative of the mole fraction to the first derivative of the concentration the following relationship is needed

$$x_A = \frac{c_A}{c} \qquad (II-47)$$

where c_A is the concentration of substance A. Taking the first derivative of equation (II-47) with respect to z remembering that c is constant yields

$$\frac{dx_A}{dz} = \frac{1}{c} \frac{dc_A}{dz} \qquad (II-48)$$

Substituting equation (II-48) into equation (II-46) gives the following expression for the concentration gradient

$$\frac{dc_A}{dz} = \frac{c(1-x_A)}{H} \ln \left(\frac{1-x_{A0}}{1-x_{AH}}\right) \qquad (II-49)$$

The concentration gradient at the surface where $x_A = x_{A0}$ becomes

$$\left.\frac{dc_A}{dz}\right|_{z=0} = \frac{c(1-x_{A0})}{H} \ln \left(\frac{1-x_{A0}}{1-x_{AH}}\right) \qquad (II-50)$$

Once the mole fraction of substance A at the liquid surface and at the top of the test cell (z = H) are known, the concentration gradient at the surface can then be calculated using equation (II-50). This analytical result can then be compared with the experimental result obtained from equation (II-37).

2. Heat Transfer Without Evaporation

It will also be shown experimentally that the interferometer can measure the one-dimensional temperature gradient at the surface of a horizontally enclosed flat plate under free convection with no evaporation of a liquid A. Again the geometry is similar to Figure 1. In this case where $\frac{dc_A}{dz} = 0$, equation (II-1) reduces to

$$\frac{dT}{dZ} = - \left[\frac{m \lambda}{3Lg\theta(n_e - n_o)} \right] \frac{RT^2}{N_B P} \qquad \text{(II-51)}$$

This equation implies that the single measurement of the fringe shift m provides the temperature gradient directly, and hence, the heat flux from the surface. In order to verify this, a theoretical check of the experimental results provided by equation (II-51) will be derived.

This case involves one-dimensional free convection from an enclosed horizontal flat plate. To obtain the temperature gradient at the surface, the heat fluxes due to conduction and convection at the surface are needed. To determine the convective heat flux, the analysis from Reference 6 (pages 534-536) will be used. This analysis develops an equation for the convective heat flux q" between two horizontally enclosed flat plates separated by a distance H apart. It was concluded that beyond a limiting thickness H, the coefficient of heat transfer by convection remains unchanged. Therefore, there should be no difference between the heat transfer through the layer H and that from a single horizontal enclosed plate facing upward. Since the height of the test cell H is large relative to the surface temperatures and thermal resistances involved in this thesis, it can be concluded that this theoretical analysis is applicable for this particular

special case. The heat flux by convection at the surface is given by

$$q'' = 0.068k \left(\frac{\beta g}{\gamma^2}\right)^{1/3} (T_1 - T_2)^{4/3} \qquad \text{(II-52)}$$

(Reference 6, page 536)

where T_1 is the temperature of the warm surface and T_2 is the temperature of the cooler air layer above.

The equation for the heat flux due to conduction at the surface is given by the Fourier-Biot Law as

$$q'' = -k \left.\frac{dT}{dz}\right|_{z=0} \qquad \text{(II-53)}$$

The heat flux due to convection and the heat flux due to conduction are equal at the heated surface due to continuity of fluxes. Setting equation (II-52) equal to equation (II-53) and solving for the temperature gradient yields

$$\left.\frac{dT}{dz}\right|_{z=0} = -0.068\left(\frac{\beta g}{\gamma^2}\right)^{1/3}(T_1 - T_2)^{4/3} \qquad \text{(II-54)}$$

Knowing $\frac{\beta g}{\gamma^2}$ for air, the temperature at the surface T_1 and the temperature of a cooler layer of air above, T_2, the temperature gradient at the surface can be calculated analytically by using equation (II-54). This analytical result can then be compared with the experimental results obtained by measuring the fringe shifts in connection with equation (II-51).

CHAPTER III

TEST EQUIPMENT

The test apparatus consisted of a differential interferometer, a one-dimensional diffusion cell instrumented with heater and thermo-couples, a special temperature control device, and a 4 inch by 5 inch still camera. This chapter provides a detailed description of the equipment. Figure 2 shows the general layout of the equipment.

The differential interferometer is an optical instrument that permits the measurement of the gradient of index of refraction. A brief description of its operation may be found in References [5] and [8] and a more detailed description in Reference [9].

A schematic diagram of the interferometer is shown in Figure 3. Light leaves the light source and passes through a filter to obtain a particular wave length. It then passes through a polarizer which produces two equal magnitude electrical vectors. These two components are focused on the first of three Wollaston prisms, WP1. The Wollaston prism causes the light rays from each electric vector to diverge as they leave the prism. The first Wollaston prism is located at the focal point of the first spherical mirror, SP1, so that after leaving the mirror the two rays have parallel but slightly different paths. The rays pass through the test section, and are then focused by a second spherical mirror, SM2, on the second Wollaston prism, WP2. The second prism is rotated 180° with respect to the first prism so that its effect is reversed, and hence the two rays are recombined into a single ray. This single ray then passes through
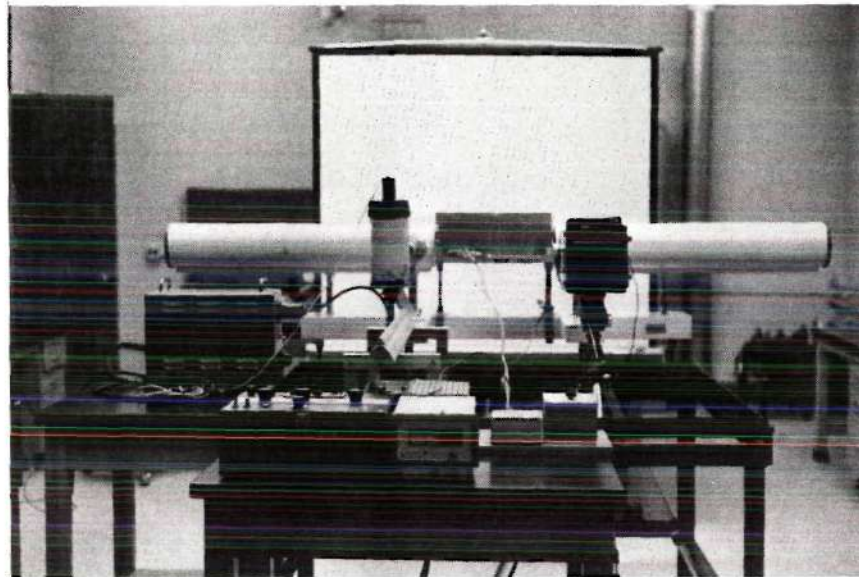
Figure 2.   Interferometer, Test Cell and
Auxilary Equipment.

PM1

Test Object

SM1

SM2

WP1

PM2

WP2

L2

P

L1

F

WP3

LS

A

E

A - Analyzer
E - Eyepiece
F - Filter
L - Lens
LS - Light Source
P - Polarizer
PM - Plane Mirror
SM - Spherical Mirror
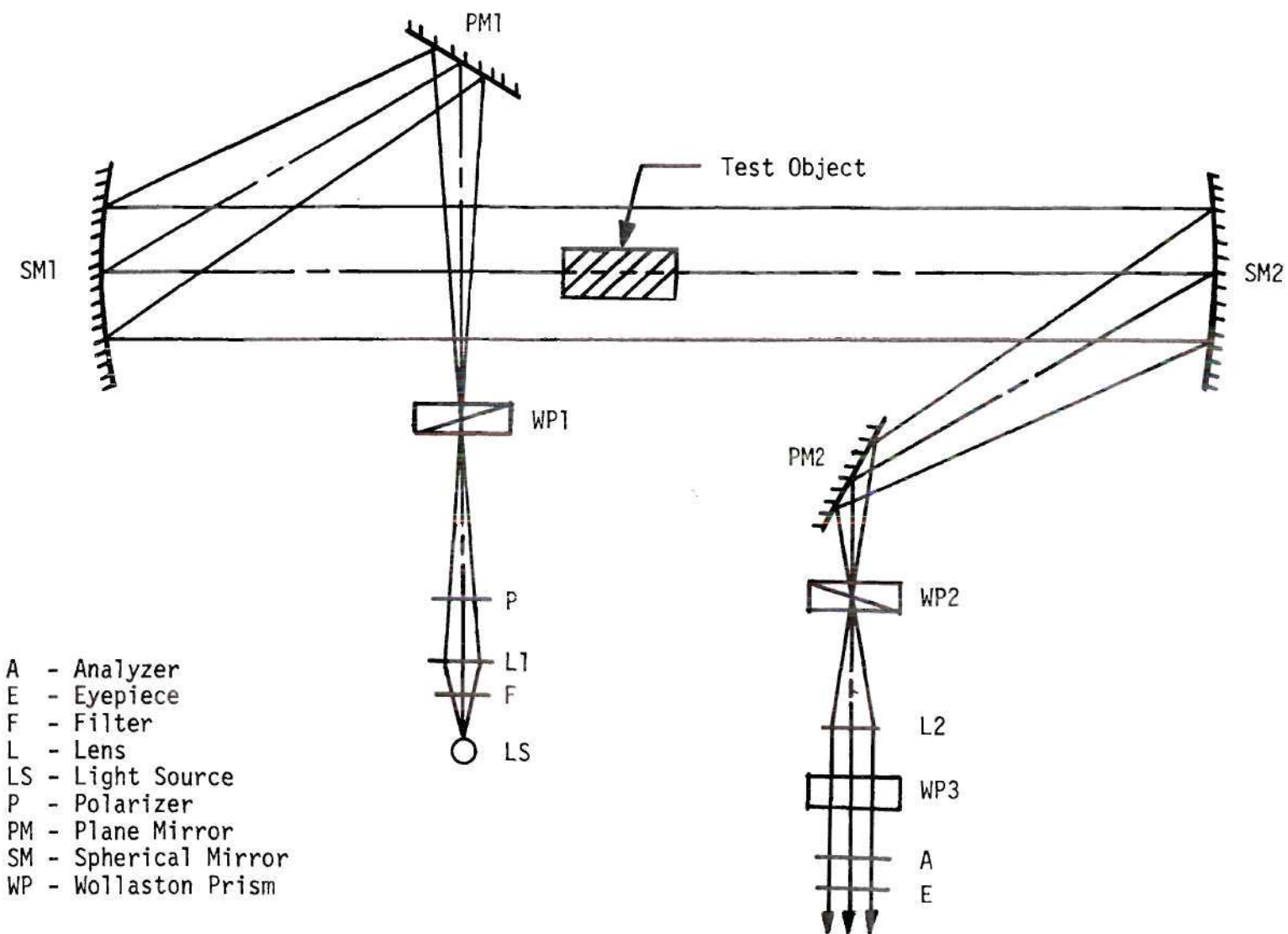WP - Wollaston Prism

26

Figure 3.   Schematic Diagram of a Differential Interferometer.

the third Wollaston prism, WP3, which produces a phase shift between the
two electric vectors. The resulting interference pattern produced by
the third Wollaston prism is a series of equally spaced parallel fringes.
These fringes are light and dark bands which are deflected in the regions
where there is a difference in optical path in the test section.

The index of refraction gradient as a function of the optical
parameters and fringe shift m given in Reference [5] is

$$\frac{\partial n}{\partial z} = [\frac{\lambda}{2Lg\theta(n_e-n_o)}]\, m \qquad\qquad (III-1)$$

Equation (III-1) can be combined with the Lorenz - Lorentz equation,
Dalton's law of partial pressures and the ideal equation of state to give
the following relationship between fringe shift m, temperature gradient
$\frac{dT}{dz}$ and concentration gradient $\frac{dc_A}{dz}$

$$m = \frac{3Lg\theta(n_e-n_o)}{\lambda}\, [(N_A-N_B)\frac{dc_A}{dz} - \frac{N_B P}{RT^2}\frac{dT}{dz}] \qquad (III-2)$$

Details of the derivation can be found in Reference [5]. Equation
(III-2) provides the relationship between $\frac{dT}{dz}$, $\frac{dc_A}{dz}$, the fringe shift m
and the optical properties of the interferometer.

The three Wollaston prisms in the interferometer each have three
separate interchangeable prisms with wedge angles of one, three and eight
degrees. Equation (III-1) shows that the number of fringe shifts m is
proportional to the Wollaston prism angle, θ. Hence, by selecting dif-
ferent prism angles the sensitivity of the interferometer can be varied.
In addition the third Wollaston prism may be removed so that the only

fringes which appear are those caused by a gradient of index of refraction in the test section. This fringe pattern is referred to as the infinite fringe pattern as opposed to the parallel fringe pattern obtained when the third Wollaston prism is used. The fringe lines in the infinite fringe pattern are proportional to lines of constant gradient and will be used in this experiment to prove that the assumed one-dimensional conditions within the test section do actually exist.

The test cell used in a study of binary gas diffusion coefficients presented in Reference [10] was modified for use in this study. The test cell body consisted of three main components, a base plate and two 25.4 mm thick aluminum vertical walls which were bolted to the base plate was machined from a single piece of 25.4 mm thick aluminum stock and contained a channel 25.4 mm wide and 6.37 mm deep. An asbestos strip 25.4 mm wide and 1.9 mm thick was placed at the bottom of the channel. This provided insulation between the heater and the test cell base plate. A 120 volt, 75 watt, Watlow silicone rubber, strip heater was placed in the channel on top of the asbestos insulation. The heater was 38.1 cm long, 25.4 mm wide and 1.27 mm thick. Aluminum foil was placed over the heater to protect it from the evaporating liquid. The aluminum foil was extended approximately 5 mm up the sides of the two vertical walls to provide a seal between the vertical walls and the base plate interface. The aluminum foil was then sealed to each of the vertical walls using a thin strip of tape. See Figure 4 for a cross-sectional view of the test cell.

One end of the channel in the base plate was sealed with a 3.18 mm thick piece of aluminum which was force fitted in place. The aluminum foil extended up the end plate 3.18 mm and was sealed with epoxy glue.
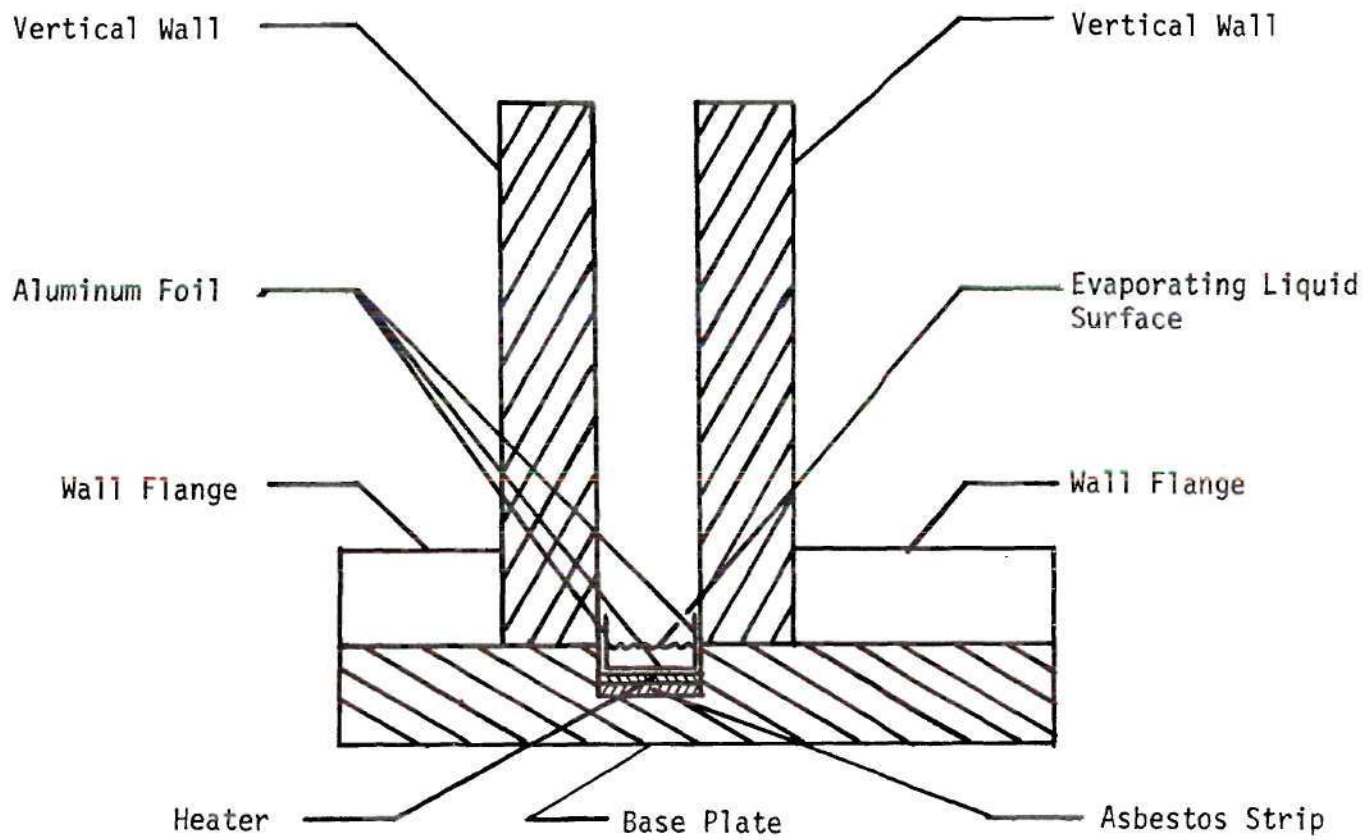
Figure 4. Cross Sectional View of Test Cell.

At the other end of the channel where the heater and wires extended beyond the end of the test cell, a 3.18 mm thick piece of aluminum was force fitted on top of the heater. The aluminum foil was then extended up the 3.18 mm high piece of aluminum and sealed with epoxy glue. This provided a trough for the test fluid which was 34.93 cm long, 25.4 mm wide and 3.18 mm deep.

The ends of the test cell were machined to provide a smooth surface to which glass end plates could be clamped. The glass end plates were poured plate glass and were 6.35 mm thick. While not optically flat, the poured plate glass end plates proved suitable for the three degree Wollaston prism setting used throughout the tests. The glass end plates were held in place at each end of the test cell using clamps.

During preliminary testing it was discovered that the warm evaporating liquid condensed on the cooler glass end plates. The condensed droplets forming on the glass end plates scattered the light, and made it impossible to measure the number of fringe shifts at the surface. To resolve this problem it was necessary to preheat the glass end plates. In order to preheat the glass, silicone rubber strip heaters were insulated on one side with asbestos strips and mounted on rigid steel strips. The heaters were 115 volt, 25 watt heaters operated on regular 110 volt outlets. The heaters were held against the outside of the glass end plates to preheat them to a temperature which would prevent the evaporating liquid from condensing. The temperature to which the glass was preheated was not recorded. The heaters were simply left on the glass long enough so that condensation did not occur during the duration of an experimental test run.

The entire test cell was mounted on the main supporting frame of the interferometer by using four threaded legs and a clamp system. The threaded legs permitted adjustment of the test cell in the field of view of the interferometer. The assembled test cell is shown on its supporting frame mounted to the interferometer in Figure 5.

The temperature control and measuring equipment consisted of five thermocouples, an automatic temperature control device, a thermocouple selector switch, a thermocouple reference junction and a potentiometer. The temperature at the surface, T_s, of the liquid was recorded and used to evaluate the vapor pressure, and hence the concentration c_A at the evaporating surface. The surface temperature was also used to evaluate the total concentration c and the diffusion coefficient D_{AB}. The temperature, T_h, at a distance h above the evaporating surface, which was set at 7.6 cm, was needed for the evaluation of equation (II-30). All physical and thermodynamic properties were evaluated at the average temperature between T_s and T_h. These properties included the thermal conductivity of the liquid vapor k_A, the thermal conductivity of air k_B, the specific heat at constant pressure of the liquid vapor c_{pA}, and the molar refractivity of air N_B.

In addition to the two thermocouples used to measure T_s and T_h, three other thermocouples were used to measure the bulk air temperature outside the test cell and the bulk fluid temperature. All thermocouples used were made from 0.127 mm diameter, teflon coated, copper-constantan wire. One thermocouple was placed in the evaporating liquid and its output was connected to the automatic temperature control device. Another thermocouple was placed at the top of the test cell which is 14.6 cm
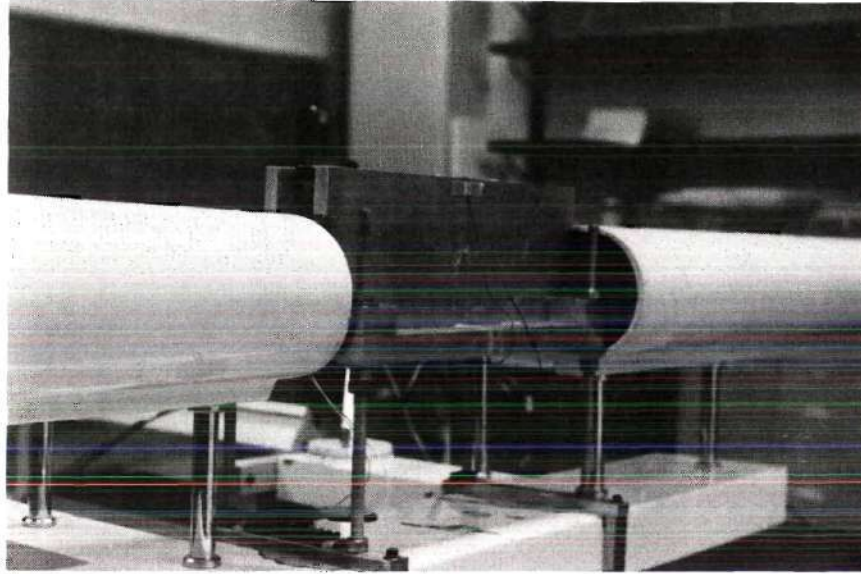
Figure 5. Test Cell on Support Stand Mounted
on the Interferometer.

above the evaporating surface. A third thermocouple was used to measure the room temperature outside the test cell. Figure 6 shows the location of the five thermocouples. The output from the three thermocouples plus the one which measured T_h were connected to the thermocouple selector switch which in turn was connected to a thermocouple reference junction and a potentiometer. The thermocouple reference junction was electrically operated and manufactured by Consolidated Ohmic Devices, Inc. in Carle Place, New York. The potentiometer was a volt potentiometer manufactured by Leeds and Northrup Co. in Philadelphia, Pennsylvania.

An automatic temperature control device manufactured by Leeds and Northrup Co. was used to automatically and continuously adjust the power into the heater so that the liquid temperature was maintained at the desired temperature. During preliminary testing two additional thermo-couples were installed at a distance of 25.4 mm from each end of the test cell. These were used to verify that the heater was providing a uniform temperature along the test cell at a distance of 1 mm above the aluminum foil in the evaporating liquid. After uniformity of temperature was verified the two extra thermocouples were removed to avoid having extra obstructions in the test cell which would hinder the one-dimensional diffusion assumption.

The camera used to record the deflected fringe lines produced by the interferometer was a Graflex, 4 inch by 5 inch, still camera. The film used was Kodak Plus-X Pan Professional Film and the shutter speed was either 1/5 or 1/10 of a second at full lens opening.
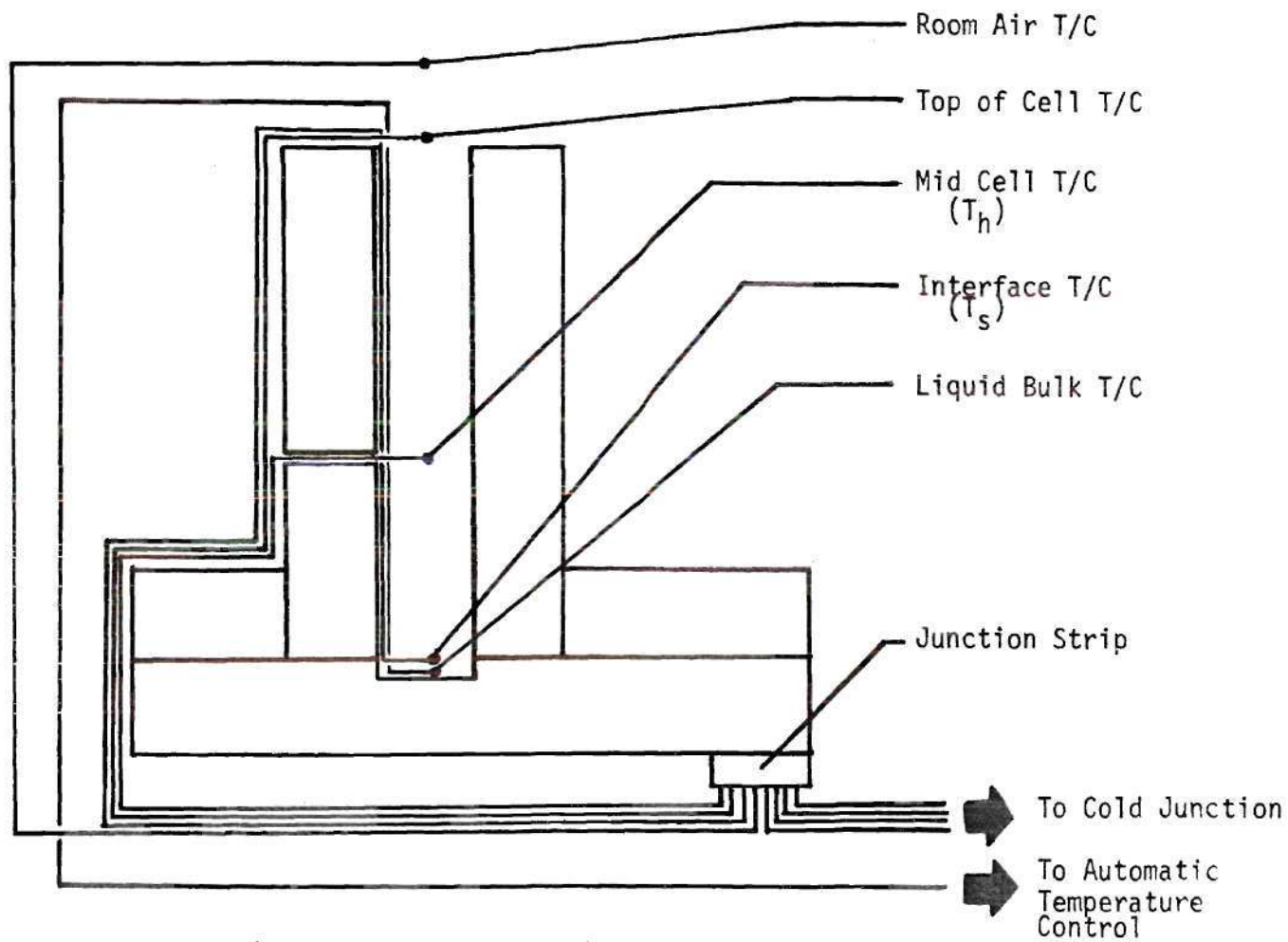
Room Air T/C

Top of Cell T/C

Mid Cell T/C
(T_h)

Interface T/C
(T_s)

Liquid Bulk T/C

Junction Strip

To Cold Junction

To Automatic
Temperature
Control

Figure 6.   Test Cell Schematic Diagram Giving
Thermocouple Locations.

CHAPTER IV

TEST PROCEDURE

This chapter provides a detailed description of the test procedure, and presents a discussion of the deficiencies and problems encountered with the test cell. Initially the test cell was aligned and leveled in the interferometer, and then locked into position for the remainder of the test procedure. At the beginning of each test the operation of the thermocouples was checked. Next, the liquid was inserted into the test cell and the automatic temperature control device was turned on to a preselected liquid bulk temperature. After steady state conditions were obtained, a photograph of the fringe pattern was taken and the thermocouple temperatures were recorded. At this point the film was developed and the data was evaluated.

The support stand consisted of four threaded legs with two nuts on each leg which could be adjusted to level the test cell in the interferometer. After the test cell was leveled the two nuts on each leg were locked against each other to hold the cell in a level position. To align the test cell it was necessary to align the vertical walls with the light passing through. This was done by observing the incidence of the light on either side of one of the vertical walls. Since the light-rays passing through the test cell were parallel, the cell was pivoted until, only a small amount of scattered light was incident on either side of the wall. At this point the upper nuts were tightened to secure the test cell in the leveled and aligned position.

Based on the size of the trough in the test cell it was deter-
mined that 27 ml of liquid should be used so that the liquid surface
would coincide with the top edges of the trough. Hence, 27 ml of
liquid was poured into a graduated cylinder and set aside.

The device used to fill the test cell was a small diameter
metal tube mounted on a block which rested on the vertical wall of the
test cell. When the device was in place, the opening of the metal tube
was just above the aluminum foil which prevented splashing and permitted
a slow gradual filling of the test cell. At the top end of the metal
tube a funnel was mounted in which the liquid could be poured.

At the beginning of each test, the thermocouples were checked to
determine if they were working properly. Initial readings were taken on
all of the thermocouples and these values were recorded. A bulk liquid
temperature was then selected and the automatic temperature control device
was set at that temperature.

The filling device was then mounted on the test cell. The auto-
matic temperature control device was turned on and at the same time the
liquid was poured into the test cell. While the system was reaching
steady state conditions, the glass end plates were heated to avoid con-
densation of the liquid. When the readings for T_s and T_h reached equilib-
rium values, it was assumed that steady state conditions existed, and the
temperatures of all the thermocouples were recorded. At the same time a
photograph was taken of the fringe shift pattern produced by the inter-
ferometer. At this point the barometric pressure was also recorded.

The film was then developed and the number of fringe shifts m were
counted and recorded. It should be noted that in order to satisfy the

sign convention associated with equation (II-1), a fringe deflection to the left corresponded to a positive m while a fringe deflection to the right corresponded to a negative m. At this point the recording of the data was complete for a particular test.

It should be mentioned that several deficiencies existed with the test cell used. First, it was very difficult to keep liquid from leaking out of the ends of the test cell. The test cell was disassembled many times and different glues and sealants were used in an attempt to eliminate the leakage. Finally a satisfactory solution involving a lip of aluminum foil bent in towards the trough was used to prevent the liquid from coming in contact with the glass end plates. Epoxy glue was then used to form a seal under the lip. This method was successful in preventing leakage of the liquid from the test cell.

The design of the test cell permitted only a limited range of liquid temperatures to be tested. The upper limit of the liquid temperature was restricted by excess heat loss from the heater to the test cell. The asbestos strip between the heater and the base plate had a lower thermal resistance than the air and liquid vapor above the heater. Hence, the heater at high temperatures tended to heat up the base plate instead of the air and liquid vapor above the heater. In addition the test cell was not capable of maintaining a constant liquid level. At high liquid temperatures the evaporation rate was so high that the liquid would completely evaporate before steady state conditions were obtained.

During preliminary testing a blower system was constructed to blow air across the top of the test cell. The blower was used in an attempt

to provide a zero concentration of the vapor at the top of the test cell as required by the boundary condition for equation (II-50) for the special case of isothermal mass transfer. However, the blower caused air currents within the test cell which disrupted the fringe pattern, and tended to cause fluctuations in the gas diffusion rate. The blower system was discarded and the diffusing vapor at the top of the cell was simply removed by normal room air currents.

Even though these problems were encountered with the test cell and supporting equipment, the necessary tests to prove the feasibility of measuring heat and mass transfer with the interferometer were performed.

CHAPTER V

RESULTS

Test results were obtained to verify the interferometer equation
(II-1) for the special cases of isothermal mass transfer, and heat trans-
fer without evaporation. For the isothermal mass transfer test, liquid
acetone was evaporated at a constant liquid surface temperature and con-
stant air temperature of $303^{\circ}K$. For the heat transfer without evapora-
tion test, a constant surface temperature of $316.5^{\circ}K$ was used. The test
results for these two special cases were then compared to their respective
theoretically predicted results. Next, test results for simultaneous heat
and mass transfer were obtained for the single liquid acetone at three
different surface temperatures between $307.4^{\circ}K$ and $312.6^{\circ}K$. For the temp-
erature range tested it was found that as the surface temperature was
increased the evaporation rate increased and in turn the heat transfer
rate decreased. An explanation of this phenomenon is presented below.
One test run was repeated four additional times to determine a measure of
consistency of the method.

Sample interferograms, both parallel fringe pattern and infinite
fringe pattern, are presented along with the test results. It should be
noted that in each case the parallel fringe pattern was used to determine
the fringe shift m. The fringe lines in the infinite fringe pattern which
correspond to lines of constant gradient were used to verify the extent
to which the one-dimensional conditions existed within the test cell. The
evaluation of the physical and optical properties used in the analysis is

presented in Appendix B.

Figures 7 and 8 show the interferograms recorded for the isothermal mass transfer case of acetone evaporating at a constant temperature of $303^{\circ}K$. Since the evaporation rate for isothermal mass transfer at room temperature is small, the eight degree Wollaston prism angle setting had to be used to provide enough sensitivity for recording the fringe deflection. Notice in Figure 7 that the fringe deflection at the surface is to the right producing a negative m. A negative fringe shift provides the proper sign for the concentration gradient in equation (II-37) which is the simplified interferometer equation for this special case. Equation (II-37) was then used to calculate the concentration gradient based on the interferometer fringe shift measurement determined from Figure 7. Equation (II-50) was used to calculate the theoretically predicted value for the concentration gradient. The mole fraction of acetone x_{AH} at the top of the cell (z = H) was assumed to be zero for the calculations. Since acetone is approximately twice as dense as air, the acetone that reached the top of the cell did not remain in the vicinity of the test cell opening and the approximation that the concentration of acetone was zero at the top was closely met. Calculations indicated that even if $x_{AH} = 0.1 \, x_{AO}$ the theoretical results would only be 8% lower than the results obtained assuming that $x_{AH} = 0$. Table 1 presents the results obtained. Equation (II-28) with $\frac{dT}{dz}$ set equal to zero was used to calculate the molar flux N_{AZ}.

Figure 7. Parallel Fringe Pattern for Isothermal
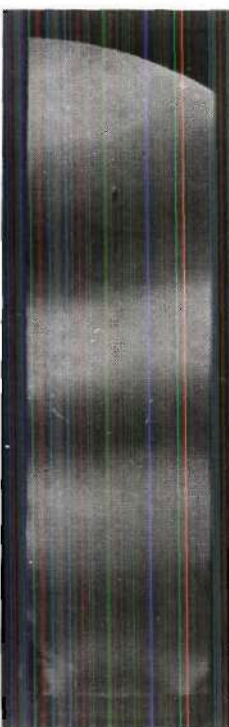Mass Transfer at $T = 303^{\circ}K$.

Figure 8. Infinite Fringe Pattern for Isothermal
Mass Transfer at $T = 303^{\circ}K$.

Table 1. Isothermal Mass Transfer Results

Method	$\frac{dc_A}{dz}$ ($\frac{moles}{cm^4}$)	N_{AZ} ($\frac{moles}{cm^2 \, sec.}$)
Experimental	-7.56×10^{-7}	1.28×10^{-7}
Theoretical	-7.78×10^{-7}	1.32×10^{-7}

Table 1 indicates that the experimental results from the interferometer are 3% lower than the theoretically predicted results for isothermal mass transfer.

Figures 9 and 10 show the interferograms recorded for the case of heat transfer without evaporation. Notice in Figure 9 that the fringe deflection at the surface is to the left producing a positive m. A positive fringe shift provides the proper sign for the temperature gradient in equation (II-51) which is the simplified interferometer equation for this special case. Equation (II-51) was then used to calculate the temperature gradient based on the interferometer fringe shift measurement determined from Figure 9. Equation (II-54) was used to calculate the theoretically predicted value for the temperature gradient. Equation (II-53) was then used to calculate the heat flux q" at the surface. Table 2 presents the results for a surface temperature of T_s = 316.5°K.

Table 2. Heat Transfer Without Evaporation Results

Method	$\frac{dT}{dz}$ ($\frac{°K}{cm}$)	$q"$ ($\frac{cal}{cm^2 \, sec.}$)
Experimental	-2.44	1.54×10^{-4}
Theoretical	-2.80	1.77×10^{-4}

Figure 9. Parallel Fringe Pattern for Heat Transfer
Without Evaporation at T_s = 316.5^{O}K.

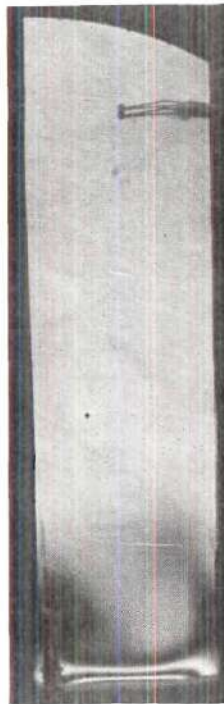

Figure 10. Infinite Fringe Pattern for Heat Transfer
Without Evaporation at T_s = 316.5^{O}K.

Table 2 indicates that the experimental results from the interferometer are 12.8% lower than the theoretically predicted results for heat transfer without evaporation.

The results for simultaneous heat and mass transfer of acetone when heated to three different temperatures will now be presented. Figures 11 and 12 show an example of interferograms recorded for the simultaneous heat and mass transfer process. Note in Figure 11 that the mass transfer is the dominating influence affecting the fringe deflection since the fringe deflection is to the right. Based on the interferometer fringe shift measurement m, and the optical and physical properties, equation (II-30) was used to calculate the temperature gradient. The fringe shift measurement m, the temperature gradient $\frac{dT}{dz}$ calculated from equation (II-30), and the optical properties were then used to calculate the concentration gradient using equation (II-29). Equation (II-53) was used to calculate the heat flux q" and Equation (II-28) was used to calculate the molar flux N_{AZ}. The results of three independent simultaneous heat and mass transfer tests are given in Table 3.

Table 3. Simultaneous Heat and Mass Transfer Results

Test	$T_s(^oK)$	$\frac{dT}{dz}$ $(\frac{^oK}{cm})$	q" $(\frac{cal}{cm^2 sec})$	$\frac{dc_A}{dz}$ $(\frac{moles}{cm^4})$	N_{AZ} $(\frac{moles}{cm^2 sec})$
1	307.4	-.172	8.41×10^{-6}	-9.71×10^{-7}	1.89×10^{-7}
2	309.3	-.168	8.07×10^{-6}	-28.8×10^{-7}	6.03×10^{-7}
3	312.6	-.084	3.87×10^{-6}	-48.1×10^{-7}	11.5×10^{-7}

Figure 11. Parallel Fringe Pattern for Simultaneous
Heat and Mass Transfer at T_s = 312.6°K.

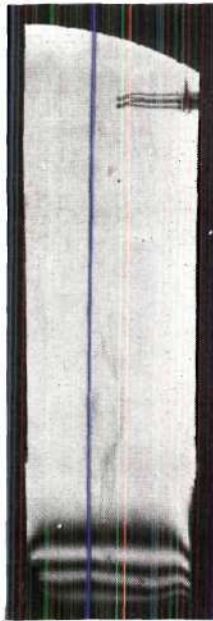

Figure 12. Infinite Fringe Pattern for Simultaneous
Heat and Mass Transfer at T_s = 312.6°K.

The results from Table 3 indicate that as the surface tempera-
ture T_S of the evaporating acetone increases, the concentration gradient
and hence molar flux increases. This trend indicates that higher sur-
face temperatures result in higher evaporation rates. It can also be
seen that as the surface temperature T_S increases during simultaneous
heat and mass transfer for the small temperature range tested that the
temperature gradient and heat flux both decrease. This trend can be
explained be referring to an equation developed in Reference [7] which
relates the heat flux with mass transfer to the heat flux without mass
transfer. This equation is

$$-k\left(\frac{dT}{dz}\right)_{z=0} = \frac{-\dfrac{N_{AZ}c_{PA}}{k}\delta}{1 - \exp\left[\left(\dfrac{N_{AZ}c_{PA}}{k}\right)\delta\right]} \left[-k\left(\frac{dT}{dz}\right)^{o}_{z=0}\right] \tag{V-1}$$

(Reference 7, eq. 18.5-9)

The terms in equation (V-1) are as follows

δ the distance above the evaporating surface where
the temperature is known (similar to h in the
analysis used in this thesis)

$-k\left(\frac{dT}{dz}\right)_{z=0}$ the heat flux at the surface with simultaneous
mass transfer

$-k\left(\frac{dT}{dz}\right)^{o}_{z=0}$ the heat flux at the surface with no mass
transfer

The other terms have been defined throughout this thesis. The exponen-
tial term in the denominator of equation (V-1) makes the factor

$$\frac{-\dfrac{N_{AZ}c_{PA}}{k}\delta}{1 - \exp\left[\dfrac{N_{AZ}c_{PA}}{k}\delta\right]} \tag{V-2}$$

less than unity. Thus for a given surface temperature T_s the heat flux with mass transfer $-k(\frac{dT}{dz})_{z=0}$ is less than the heat flux without mass transfer $-k(\frac{dT}{dz})^0_{z=0}$ according to equation (V-1). It is known and has been illustrated in this thesis in Table 3 that as the surface temperature T_s is increased, the molar flux N_{AZ} increases. However, N_{AZ} increases at a much faster rate with increasing surface temperature than does the heat flux. Table 4 indicates that in changing the surface temperature from T_s = 307.4°K in test 1 to T_s = 312.6°K in test 3 the increase in surface temperature is only 5.2°K, but the molar flux N_{AZ} is six times larger. Since N_{AZ} was six times larger for test 3 than for test 1, the factor (V-2) was much smaller for test 3 as indicated in Table 4. It can then be concluded from equation (V-1) that the heat flux and hence temperature gradient for test 3 should be less than that obtained for test 1.

Table 4. Comparison of Variation in Heat
Flux with Temperature

Test Number From Table 3	T_s (°K)	N_{AZ} ($\frac{moles}{cm^2 sec}$)	Eq. (V-2)	q" ($\frac{cal}{cm^2 sec}$)
1	307.4	1.89×10^{-7}	.753	8.41×10^{-6}
3	312.6	11.5×10^{-7}	.106	3.87×10^{-6}

An addition factor also can be given to help explain the trend for the heat flux to decrease with increasing surface temperature. This reason is related to the magnitudes of the thermal conductivities involved. The thermal conductivity of acetone vapor, k_A, at 310°K is 1222 $\frac{g-cm}{sec^3 \, °K}$

while the thermal conductivity of air, k_B, at 310^OK is $2687 \frac{g\text{-}cm}{sec^{3}\,^O K}$.
It can be seen that the thermal conductivity of air is approximately
2.2 times larger than the thermal conductivity of acetone vapor. Hence,
acetone vapor has a higher thermal resistance than does air. As the sur-
face temperature is increase causing the evaporation rate to increase
there is a higher concentration of acetone vapor immediately above the
evaporating surface in test 3 than in test 1. Since there is more acetone
vapor and less air near the evaporating surface in test 3, there is a
correspondingly larger thermal resistance which results in a lower heat
flux.

The results in test 3 for simultaneous heat and mass transfer were
repeated four additional times to assure a degree of repeatability. The
results are presented in Table 5.

Table 5. Repeatability Results

T_s (^{O}K)	$\frac{dT}{dz}$ ($\frac{^O K}{cm}$)	q'' ($\frac{cal}{cm^2 sec}$)	$\frac{dc_A}{dz}$ ($\frac{moles}{cm^4}$)	N_{AZ}($\frac{moles}{cm^2 sec}$)
312.6	-.084	3.87×10^{-6}	48.1×10^{-7}	11.5×10^{-7}
312.8	-.078	3.58×10^{-6}	49.1×10^{-7}	11.7×10^{-7}
312.6	-.081	3.72×10^{-6}	48.1×10^{-7}	11.5×10^{-7}
312.6	-.075	3.45×10^{-6}	48.1×10^{-7}	11.5×10^{-7}

CHAPTER VI

CONCLUSIONS AND RECOMMENDATIONS

A method has been developed for the experimental measurement of simultaneous heat and mass transfer. The method utilizes a single interferometer fringe shift measurement along with various optical and physical properties to determine the simultaneous heat and mass transfer rates for a one-dimensional binary gas diffusion in free convection. Initially results were obtained to verify that the differential interferometer could measure the evaporation rate for isothermal mass transfer, and could also measure the heat flux for heat transfer without evaporation. Next, results were obtained for simultaneous heat and mass transfer of the liquid acetone at three different surface temperatures. No attempt was made to check the experimental values for simultaneous heat and mass transfer with theoretical results because of the complexity in a theoretical analysis. However, one of the three tests was repeated four times which resulted in insignificant variations in the measured values for heat and mass transfer rates.

It can be concluded that the method presented here for using the differential interferometer to measure simultaneous heat and mass transfer rates is superior to the methods suggested in References [3] and [4]. The two-wavelength Mach-Zehnder interferometer technique [3] requires that the variation in the molar refractivity with respect to wavelength is large so that the variation on fringe shift is sensitive enough to

produce independent results. With the technique developed for the differential interferometer this is not a problem. An additional problem with the Mach-Zehnder interferometer techniques is the difficulty of photographing the interference pattern simultaneously at two different wave lengths. Again with the differential interferometer this problem does not exist because only a single photograph is necessary.

It can also be concluded that the differential interferometer technique has an advantage over the one wavelength Mach-Zehnder interferometer technique presented in Reference [4]. The Mach-Zehnder interferometer produces fringe lines which are identical to isotherms for heat transfer or lines of constant concentration for mass transfer. In order to determine the temperature gradient, for example, one must approximate the temperature gradient by knowing the location of the isotherms. However, with the differential interferometer the fringe shift measurement is directly proportional to the temperature and concentration gradients and the graphical determination of the slopes of these profiles is unnecessary.

The major effort of this thesis was to develop a technique applicable to a differential interferometer for measuring simultaneous heat and mass transfer rates. This objective has been accomplished, however, due to the many problems encountered with the test cell, it is recommended that further testing be performed with a redesigned test cell. In addition a wider temperature range should be used during the measurement phase and measurements should be extended for additional substances.

Some recommendations for redesigning the test cell are as follows:

1. A thin sheet of aluminum should be used to make a trough for the liquid with the ends of the trough welded to prevent leakage. Ample insulation should be placed between the heater and the base plate which holds the trough to allow higher temperatures to be tested.

2. A device should be designed to maintain the liquid at a constant level inside the aluminum trough. The device should be capable of preheating the liquid to the surface temperature being tested prior to the liquid flowing into the trough. This device will permit testing at higher surface temperatures without worrying about total evaporation of the liquid prior to reaching steady state conditions.

3. The method used in this thesis to prevent liquid vapor from condensing on the glass end plates was not considered the best method. A better method would have been to install heater wires within the glass when they were poured. The heat could then be controlled properly and could be confined to the base of the glass plate only.

4. A hygrosensor should be placed at the top of the test cell to measure the concentration of the vapor of the evaporating liquid. This would help in the theoretical verification of the isothermal mass transfer case.

APPENDICES

APPENDIX A

THE "B" COEFFICIENTS OF EQUATION (II-16)

The third degree algebraic equation (II-16) relating the temperature gradient to the concentration gradient contained the coefficients B_1 through B_5. Equation (II-16) was

$$B_1 \left(\frac{\partial T}{\partial z}\right)^3 + B_2 \left(\frac{\partial c_A}{\partial z}\right)^3 + B_3 \left(\frac{\partial T}{\partial z}\right)^2 \left(\frac{\partial c_A}{\partial z}\right) + B_4 \left(\frac{\partial c_A}{\partial z}\right)^2 \left(\frac{\partial T}{\partial z}\right) + B_5 = 0$$

The coefficients B_1 through B_5 are as follows (pages 54-56):

$$B_1 = -\frac{\rho c_A^2 D_{AB}^2 P^3}{(c-c_A)^2 R^3 T^6}(M_A^2 M_B) + \left[\frac{4\mu\rho c_{PA} c_A^2 D_{AB}^2 P^3}{3k(c-c_A)^2 R^3 T^6}\right.$$

$$+ \frac{8\mu\rho c_A D_{AB} P^2}{3(c-c_A) R^2 T^5} + \frac{4\mu\rho c_A^2 D_{AB} P}{3k(c-c_A) R T^3}\left(\frac{\partial \kappa_A}{\partial T} - \frac{\partial \kappa_B}{\partial T}\right)$$

$$+ \frac{4\mu\rho c_A D_{AB} P^2}{3k(c-c_A) R^2 T^4}\frac{\partial \kappa_B}{\partial T} + \frac{4\mu\rho c_A^2 D_{AB} P}{3k(c-c_A) R T^4}(\kappa_A-\kappa_B)$$

$$- \frac{4\rho c_A^2 D_{AB} P}{3(c-c_A) R T^3}\left(\frac{\partial \mu_A}{\partial T} - \frac{\partial \mu_B}{\partial T}\right) - \frac{4\rho c_A D_{AB} P^2}{3(c-c_A) R^2 T^4}\frac{\partial \mu_B}{\partial T}$$

$$- \frac{4\rho c_A^2 D_{AB} P}{3(c-c_A) R T^4}(\mu_A-\mu_B)\bigg](M_A M_B) - \frac{8\mu c_A D_{AB} P^3}{3(c-c_A) R^3 T^6}(M_A M_B^2)$$

$$+\left[\frac{4\mu\rho c_A^3 c_{PA} D_{AB}^2 P^2}{3k(c-c_A)^2 R^2 T^5} + \frac{8\mu\rho c_A^2 D_{AB} P}{3(c-c_A) R T^4} - \frac{4\mu\rho c_A^2 D_{AB} P^2}{3(c-c_A)^2 R^2 T^5}\right.$$

$$- \frac{4\mu\rho c_A^2 P}{3(c-c_A)^2 R T^3}\frac{\partial D_{AB}}{\partial T} + \frac{4\mu\rho c_A^3 D_{AB}}{3k(c-c_A) T^2}\left(\frac{\partial \kappa_A}{\partial T} - \frac{\partial \kappa_B}{\partial T}\right)$$

$$+ \frac{4\mu\rho c_A^2 D_{AB} P}{3k(c-c_A) R T^3}\frac{\partial \kappa_B}{\partial T} + \frac{4\mu\rho c_A^3 D_{AB}}{3k(c-c_A) T^3}(\kappa_A-\kappa_B)\bigg](M_A^2$$

$$- M_A M_B)$$

$$B_2 = \frac{\rho D_{AB}^2 P^2}{(c-c_A)^2 R^2 T^2}(M_A^3 - M_A^2 M_B) + \left[\frac{4\mu\rho D_{AB} P}{3(c-c_A)^2 R T}\right.$$

$$- \frac{4\rho D_{AB}}{3(c-c_A)}(\mu_A-\mu_B)\bigg](M_A M_B - M_A^2)$$

$$+ \frac{8\mu D_{AB} P}{3(c-c_A) R T}(2M_A^2 M_B - M_A^3 - M_A M_B^2)$$

$$B_3 = -\frac{2\rho c_A D_{AB}^2 P^3}{(c-c_A)^2 R^3 T^5}(M_A^2 M_B) - \frac{8\mu D_{AB} P^3}{3(c-c_A) R^3 T^5}(M_A M_B^2)$$

$$+\left[\frac{8\mu\rho C_{PA} c_A D_{AB}^2 P^3}{3K(c-c_A)^2 R^3 T^5} + \frac{8\mu\rho D_{AB} P^2}{3(c-c_A) R^2 T^4}\right.$$

$$+\frac{4\mu\rho c_A D_{AB} P}{3K(c-c_A) R T^2}\left(\frac{\partial k_A}{\partial T} - \frac{\partial k_B}{\partial T}\right) + \frac{4\mu\rho D_{AB} P^2}{3K(c-c_A) R^2 T^3}\frac{\partial k_B}{\partial T}$$

$$+\frac{8\mu\rho c_A D_{AB} P}{3K(c-c_A) R T^3}(k_A - k_B) - \frac{4\rho c_A D_{AB} P}{3(c-c_A) R T^2}\left(\frac{\partial \mu_A}{\partial T} - \frac{\partial \mu_B}{\partial T}\right)$$

$$-\frac{4\rho D_{AB} P^2}{3(c-c_A) R^2 T^3}\frac{\partial \mu_B}{\partial T} - \frac{8\rho c_A D_{AB} P}{3(c-c_A) R T^3}(\mu_A - \mu_B)\right](M_A M_B)$$

$$+\frac{\rho c_A^2 D_{AB}^2 P^2}{(c-c_A)^2 R^2 T^4}(M_A^3 - M_A^2 M_B) + \left[\frac{8\mu\rho C_{PA} c_A^2 D_{AB}^2 P^2}{3K(c-c_A)^2 R^2 T^4}\right.$$

$$+\frac{8\mu\rho c_A D_{AB} P}{3(c-c_A) R T^3} - \frac{8\mu\rho c_A D_{AB} P^2}{3(c-c_A)^2 R^2 T^4} - \frac{8\mu\rho c_A P}{3(c-c_A) R T^2}\frac{\partial D_{AB}}{\partial T}$$

$$+\frac{4\mu\rho c_A^2 D_{AB}}{3K(c-c_A) T}\left(\frac{\partial k_A}{\partial T} - \frac{\partial k_B}{\partial T}\right) + \frac{4\mu\rho c_A D_{AB} P}{3K(c-c_A) R T^2}\frac{\partial k_B}{\partial T}$$

$$+\frac{8\mu\rho c_A^2 D_{AB}}{3K(c-c_A) T^2}(k_A - k_B) - \frac{4\mu\rho c_A^2 D_{AB} P}{3(c-c_A)^2 R T^3}$$

$$+\frac{4\rho c_A^2 D_{AB}}{3(c-c_A) T}\left(\frac{\partial \mu_A}{\partial T} - \frac{\partial \mu_B}{\partial T}\right) + \frac{4\rho c_A D_{AB} P}{3(c-c_A) R T^2}\frac{\partial \mu_B}{\partial T}$$

$$+\frac{4\rho c_A^2 D_{AB}}{3(c-c_A) T^2}(\mu_A - \mu_B)\right](M_A^2 - M_A M_B)$$

$$+\frac{16\mu c_A D_{AB} P^2}{3(c-c_A) R^2 T^4}(M_A^2 M_B - M_A M_B^2)$$

$$B_4 = -\frac{e D_{AB}^2 P^3}{(c-c_A)^2 R^3 T^4}(M_A^2 M_B) + \left[\frac{4\mu e c_{PA} D_{AB}^2 P^3}{3K(c-c_A)^2 R^3 T^4}\right.$$

$$+ \frac{4\mu e D_{AB} P}{3K(c-c_A) R T^2}(\kappa_A - \kappa_B) - \frac{4 e D_{AB} P}{3(c-c_A) R T^2}(\mu_A - \mu_B)\left.\right](M_A M_B)$$

$$+ \frac{2 e c_A D_{AB} P^2}{(c-c_A)^2 R^2 T^3}(M_A^3 - M_A^2 M_B) + \left[\frac{4\mu e c_{PA} c_A D_{AB}^2 P^2}{3K(c-c_A)^2 R^2 T^3}\right.$$

$$- \frac{4\mu e D_{AB} P^2}{3(c-c_A)^2 R^2 T^3} - \frac{4\mu e c_A D_{AB} P}{3(c-c_A)^2 R T^2} - \frac{4\mu e P}{3(c-c_A) R T}\frac{\partial D_{AB}}{\partial T}$$

$$+ \frac{4\mu e c_A D_{AB}}{3(c-c_A) K T}(\kappa_A - \kappa_B) + \frac{4 e c_A D_{AB}}{3(c-c_A)}\left(\frac{\partial \mu_A}{\partial T} - \frac{\partial \mu_B}{\partial T}\right)$$

$$+ \frac{4 e D_{AB} P}{3(c-c_A) R T}\frac{\partial \mu_B}{\partial T} + \frac{8 e c_A D_{AB}}{3(c-c_A) T}(\mu_A - \mu_B)$$

$$- \frac{4\mu e c_A D_{AB} P}{3(c-c_A)^2 R T^2}\left.\right](M_A^2 - M_A M_B) + \frac{16\mu D_{AB} P^2}{3(c-c_A) R^2 T^3}$$

$$(M_A^2 M_B - M_A M_B^2) + \frac{8\mu c_A D_{AB} P}{3(c-c_A) R T^2}(2 M_A^2 M_B - M_A^3$$

$$- M_A M_B^2)$$

$$B_5 = \rho^4 \bar{g}_z$$

APPENDIX B

EVALUATION OF PHYSICAL AND OPTICAL PROPERTIES

Various physical and optical properties are needed in order to
evaluate equations (II-29) and (II-30). The method of calculating these
properties and the references used are presented as follows.

Constant Optical Properties

Several of the optical properties remained constant for all of
the tests. They are:

L = 35.66 cm = test cell length

g = 100 cm = focal length of the spherical mirrors in
the differential interferometer

n_e-n_o = 0.00911 = difference in index of refraction of
the extraordinary and ordinary rays in
the Wollaston Prism material

λ = 5820Å = test wavelength

θ = 0.05236 Radians = Wollaston Prism angle for 3° setting

θ = 0.13963 Radians = Wollaston Prism angle for 8° setting.

The test cell length was determined by measuring the distance
between the two glass end plates when the test cell was assembled. The
mirror focal length, the index of refraction difference and the test
wavelength were obtained from technical information about the interferom-
eter supplied by the manufacturer in Reference [11]. The three degree
Wollaston Prism angle setting was determined by preliminary testing to
be the best setting for the work performed in this thesis except for the

special isothermal mass transfer case where the eight degree setting
was used.

Molar Refractivities

The molar refractivity of acetone, N_A, was calculated using the
Lorenz-Lorentz Equation in the form

$$N_A = \left(\frac{n_A^2 - 1}{n_A^2 + 2} \right) \frac{M_A}{\rho_A} \qquad \text{(B-1)}$$

Since the molar refractivity is very nearly independent of phase, temp-
erature and pressure, liquid phase data can be used to determine values
for the vapor phase. Data for the index of refraction and density of
acetone were available from Reference [12]. The optical data was pre-
sented at four wavelengths, 4340.6Å, 4861.5Å, 5893.0Å, and 6563.0Å for
acetone in the liquid state. To determine the molar refractivity at the
test wavelength of $\lambda = 5820.0$Å, the molar refractivity at the four given
wavelengths was calculated using equation (B-1) and plotted. The molar
refractivity at the test wavelength was then interpolated from the graph.

The molar refractivity of air, N_B, was also calculated from the
Lorenz-Lorentz equation for air which is

$$N_B = \left(\frac{N_B^2 - 1}{N_B^2 + 2} \right) \frac{RT}{P} \qquad \text{(B-2)}$$

The index of refraction for air, n_B, is dependent upon the air temper-
ature, pressure and relative humidity. The correction factor for temp-
erature and pressure is given by Reference [13] to be

$$(n_{DB} - 1)_{T,P} = (n_{DB} - 1)_r \frac{P}{P_r} \frac{T_r}{T} \qquad (B-3)$$

The correction factor for the relative humidity from Reference [13] is

$$(n_B - 1) = (n_{DB} - 1) - \frac{0.41 \ x_{wv}}{10^4} \qquad (B-4)$$

Combining equations (B-1), (B-2) and (B-3) yields

$$n_B = 1 + (n_{DB} - 1)_r \frac{P}{P_r} \frac{T_r}{T} - \frac{0.41 \ P_{wv}}{10^4 \ P} \qquad (B-5)$$

Equation (B-5) gives the index of refraction of air corrected for temperature, pressure and the presence of water vapor in the air. The index of refraction for dry air at a reference temperature of $288°K$ and a reference pressure of 760 mm for the interferometer wavelength used is 0.00027658 from Reference [13]. Assuming that

$$\frac{n^2 - 1}{n^2 + 2} \cong \frac{2}{3} (n-1) \qquad (B-6)$$

The Lorenz-Lorentz equation (B-2) corrected for temperature, pressure and humidity becomes

$$N_B = \frac{2\bar{R}T_B}{3P} [0.00027658 \ \frac{P}{(760)} \frac{288}{T_B} - \frac{0.41 \ P_{wv}}{10^4 \ P}] \qquad (B-7)$$

Equation (B-7) was used to calculate the molar refractivity of air.

Thermal Conductivity

Data [14] for the thermal conductivity of acetone vapor, k_A, and for air, k_B, as a function of temperature was plotted over the temperature range used for the testing in the experimental phase. The thermal conductivity of the system, k, for a particular temperature was calculated from the following relationship

$$k = \frac{c_A}{c} k_A + \frac{c - c_A}{c} k_B \qquad (B-8)$$

Specific Heat

Data for the specific heat at constant pressure for acetone vapor, c_{PA}, as a function of temperature was taken from Reference [15]. The data was plotted over the temperature range needed for this thesis.

Vapor Pressure of Acetone

Data for the vapor pressure of acetone, P_{VAP}, as a function of temperature was taken from Reference [16]. The data was plotted over the temperature range needed for the work in this thesis

Mass Diffusivity

A value for the mass diffusivity, D_{AB}, of acetone vapor in air was found to be 0.107 cm^2/sec at a temperature of 25°C and a pressure of 760 mm Hg from References [17] and [18]. The following equation from Reference [19] was used to calculate the mass diffusivity as a function of temperature

$$D_{AB} = \frac{0.001858 T^{3/2} \left(\frac{M_A + M_B}{M_A M_B}\right)^{1/2}}{P \sigma_{AB}^2 \Omega_D} \qquad \text{(B-9)}$$

where σ_{AB} is the Lennard-Jones force constant for the mixture and Ω_D is the Lennard-Jones potential function. Both Ω_P and σ_{AB} were determined from information presented in tables in Reference [19]. The mass diffusivity was then calculated for the temperatures needed using equation (B-9).

Gas Constant

The universal gas constant taken from reference [7] is

$$\bar{R} = 82.05 \; \frac{cm^3 \; atm}{g\text{-mole} \; {}^\circ K}$$

BIBLIOGRAPHY

1. Ross, P. A., and El-Wakil, M. M., "A Two Wavelength Interferometric Technique for the Study of Vaporization and Combustion of Fuels," _Progress of Astronautic and Rocketry,_ Vol. 2, 1960, pp. 265-298.

2. El-Wakil, M. M. and Jaeck, C. L., "A Two-Wavelength Interferometer for the Study of Heat and Mass Transfer," _Transactions of the ASME,_ August 1964. pp. 464-466.

3. Sadovnikov, G. V., Smol'skiy, B. M., and Shchitnikov, V. K., "Investigation of Simultaneous Heat and Mass Transfer using an Interferometer," _Heat Transfer,_ Soviet Research, Vol. 1, No. 1, 1969.

4. Prasad, C., Chen., C. S., and Beard, J. T., "An Interferometric Technique for Temperature and Concentration Measurement for an Air-Water Interface," ASME Paper No. 70-WA/Temp-1, presented at the Winter Annual Meeting, New York, New York, November 29-December 3, 1970.

5. Black, W. Z. and Carr, W. W., "A Differential Interferometer and its Application to Heat and Mass Transfer Measurements," ASME Paper No. 72-HT-12, presented at the ASME-AICHE Heat Transfer Conference, Denver, Colorado, August, 1972.

6. Jakob, L. M., _Heat Transfer,_ John Wiley and Sons, Inc., New York, c. 1949.

7. Bird, R. B., Stewart, W. E. and Lightfoot, E. N., _Transport Phenomena,_ John Wiley and Sons, Inc., New York, c. 1960.

8. Black, W. Z. and Carr, W. W., "Application of a Differential Interferometer to the Measurement of Heat Transfer Coefficients," _The Review of Scientific Instruments,_ Vol. 42, pp. 337-340, 1971.

9. Carr, W. W., "The Measurement of Instantaneous, Local Heat Transfer from a Horizontally Vibrating Isothermal Cylinder Using a Differential Interferometer," Doctor of Philosophy Thesis, Georgia Institute of Technology, 1973.

10. Somers, R. L., "An Interferometric Method for the Determination of Binary Diffusion Coefficients," Master of Science Thesis, Georgia Institute of Technology, 1974.

11. Schrader, W., _Differential Interferometer,_ WSW Fine Instruments and Optics, Wenden, Germany, April 1960.

12. Washborn, E. W., Editor, International Critical Tables of Numerical Data, Physics, Chemistry and Technology, McGraw-Hill Book Company, Inc., New York, N. Y., c. 1926.

13. Weast, R. C., Editor, Handbook of Chemistry and Physics, 51st Edition, Chemical Rubber Company, Cleveland, Ohio, 1970-1971.

14. Touloukian, Y. S. Liley, P. E., and Soxena, S. C., "Thermal Conductivity," Thermophysical Properties of Matter, Volume 3, New York: IFI/Plenum, 1970.

15. Touloukian, Y. S., Liley, P. E., and Soxena, S. C. "Specific Heat," Thermophysical Properties of Matter, Volume 6, New York: IFI/Plenum, 1970.

16. Perry, R. H. Chilton, C. H., and Kirkpatrick, S. D. Editors, Chemical Engineers Handbook, Fourth Edition, McGraw Hill Book Company, New York, 1963.

17. Lugg, G. A. "Diffusion Coefficients of Some Organic and Other Vapors in Air," Analytical Chemistry, Vol. 40, No. 7, pp. 1072-1077, June 1968.

18. Richardson, J. F., "The Evaporation of Two-Component Liquid Mixtures," Chemical Engineering Science, Vol. 10, pp. 234-242, 1959.

19. Reid, R. C. and Sherwood, T. K., The Properties of Gases and Liquids, Second Edition, McGraw Hill Book Company, New York, 1966.